

## High-speed 1.55 $\mu\text{m}$ operation of low-temperature-grown GaAs-based resonant-cavity-enhanced $p-i-n$ photodiodes

B. Butun, N. Biyikli,<sup>a)</sup> I. Kimukin, O. Aytur, and E. Ozbay  
*Department of Physics, Bilkent University, Bilkent Ankara 06800, Turkey*

P. A. Postigo, J. P. Silveira, and A. R. Alija  
*Instituto de Microelectrónica de Madrid, Isaac Newton 8, 28760 Tres Cantos, Madrid, Spain*

(Received 10 December 2003; accepted 31 March 2004; published online 6 May 2004)

We report the design, growth, fabrication, and characterization of GaAs-based high-speed  $p-i-n$  photodiodes operating at 1.55  $\mu\text{m}$ . A low-temperature-grown GaAs (LT-GaAs) layer was used as the absorption layer and the photoresponse was selectively enhanced at 1.55  $\mu\text{m}$  using a resonant-cavity-detector structure. The bottom mirror of the resonant cavity was formed by a highly reflecting 15-pair GaAs/AlAs Bragg mirror. Molecular-beam epitaxy was used for wafer growth, where the active LT-GaAs layer was grown at a substrate temperature of 200 °C. The fabricated devices exhibited a resonance around 1548 nm. When compared to the efficiency of a conventional single-pass detector, an enhancement factor of 7.5 was achieved. Temporal pulse-response measurements were carried out at 1.55  $\mu\text{m}$ . Fast pulse responses with 30 ps pulse-width and a corresponding 3 dB bandwidth of 11.2 GHz was measured. © 2004 American Institute of Physics. [DOI: 10.1063/1.1756208]

High-performance photodetectors operating in the 1.3–1.6  $\mu\text{m}$  range are vital components for long-haul optical fiber communication systems.<sup>1,2</sup> Conventional GaAs-based photodetectors however, can only operate in the first optical communication window ( $\lambda \sim 0.85 \mu\text{m}$ ) due to low cut-off wavelength. To overcome this limitation and to use GaAs-based detectors in the 1.3–1.6  $\mu\text{m}$  wavelength region, mainly two detector structures were offered: Schottky-barrier internal photo-emission photodetectors and low-temperature-grown GaAs (LT-GaAs)-based photodetectors.<sup>3,4</sup> It was shown that LT-GaAs was able to absorb long-wavelength signals due to midgap defects or As precipitates.<sup>5</sup> Moreover, subpicosecond carrier trapping time in LT-GaAs was also demonstrated.<sup>6–8</sup> Combining these two unique properties, LT-GaAs-based high-speed photodetectors operating in the 1.3–1.6  $\mu\text{m}$  range have been reported.<sup>9,10</sup>

The long-wavelength (below-bandgap) absorption coefficient of LT-GaAs is much smaller than the interband absorption coefficient.<sup>11</sup> This leads to poor efficiency performance with conventional single-pass vertical detector structures.<sup>12</sup> To overcome the problem of low efficiency, edge-coupled LT-GaAs waveguide photodetectors were proposed and successfully demonstrated.<sup>10</sup> Another method for improving the device efficiency is to use a resonant cavity enhanced (RCE) detector structure. With this structure, the detector efficiency is selectively enhanced at the resonance wavelengths of the resonant cavity.<sup>13</sup> Several groups have reported high-performance photodetectors using RCE detection scheme.<sup>14–18</sup> This technique can also be used to improve the efficiency performance of LT-GaAs-based photodetectors. Previously, we had demonstrated GaAs-based RCE Schottky-barrier internal photoemission photodetector operating at 1.3  $\mu\text{m}$ .<sup>3</sup> In this work we demonstrate LT-GaAs

based RCE photodetectors with high-speed operation at 1.55  $\mu\text{m}$ .

The optical design of the photodiode wafer was accomplished by using transfer matrix method (TMM) based theoretical simulations. Spectral reflectivity and responsivity simulations were carried out to find the desired epitaxial structure. The RCE  $p-i-n$  photodiode was designed to achieve a resonance at 1.55  $\mu\text{m}$ . In order to meet this resonance condition, a highly reflecting 15 pair GaAs/AlAs Bragg mirror centered at 1.55  $\mu\text{m}$  was designed as the bottom mirror of the detector cavity. The air/GaAs interface acted as the top mirror for the resonant cavity. The cavity layers in between were formed by GaAs layers. To eliminate the standing wave effect in the resonant cavity, thickness of the active LT-GaAs layer was designed as an integer multiple of  $\lambda/2$ .<sup>13</sup> Except for the lightly absorptive LT-GaAs layer, all layers were transparent around the operation wavelength of 1.55  $\mu\text{m}$ . A schematic of the designed RCE photodiode structure is shown in Fig. 1(a).

Samples were grown on 3 in. semi-insulating GaAs wafers (001) by molecular beam epitaxy. After thermal oxide desorption, a 0.15  $\mu\text{m}$  GaAs buffer layer was grown before the bottom GaAs/AlAs Bragg reflector. The reflector consisted of 15 pairs of undoped GaAs (113.6 nm) and AlAs (134.3 nm) layers grown with a substrate temperature  $T_s = 600$  °C. On top of the reflector an undoped GaAs layer (300 nm) was grown at  $T_s = 550$  °C and two  $n$ -type GaAs:Si layers with  $n^+ = 2 \times 10^{18} \text{ cm}^{-3}$  (300 nm) and  $n^- = 1 \times 10^{16} \text{ cm}^{-3}$  (300 nm) were grown at the same substrate temperature.  $\text{As}_4$  flux was kept at  $1 \times 10^{-5}$  mbar during all the growth ( $\text{As}_4/\text{Ga}$  flux ratio around 25). Reflection high-energy electron diffraction (RHEED) pattern was streaky along the growth of the mirror. The substrate temperature was decreased to 200 °C for the growth of the 500-nm-thick lightly doped LT section of the detector ( $n^- = 1 \times 10^{16}$

<sup>a)</sup>Electronic mail: biyikli@ee.bilkent.edu.tr

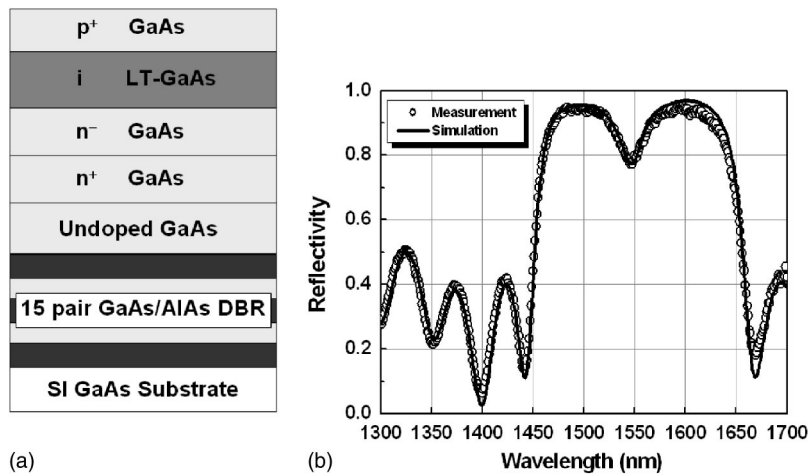


FIG. 1. (a) Epitaxial structure of the RCE  $p-i-n$  photodiode. (b) Measured and simulated spectral reflectivity of the grown RCE  $p-i-n$  photodetector wafer.

$\text{cm}^{-3}$ ). During this stage the RHEED showed a slightly hazy pattern and a decrease in the diffracted intensity with time, but still showing long lines. We attribute this RHEED pattern to an increment of the surface roughness due to the excess As present on the surface. After this layer the substrate temperature was increased again to  $T_s=550^\circ\text{C}$  and a streaky and clearly defined RHEED ( $2\times 4$ ) pattern was recovered during the growth of the top  $p$ -type GaAs:Be layer ( $p^+=1\times 10^{19}$ , 330 nm). To compare the performance of the RCE photodiode samples with conventional single-pass photodiodes, a nonresonant detector wafer was also grown with the same growth parameters except the bottom Bragg mirror.

After wafer growth, spectral reflectivity of the samples was measured using an optical spectrum analyzer in combination with a fiber-optic based reflectivity probe. The measured spectral reflectivity was compared with the TMM-based simulation results. Figure 1(b) shows the measured and simulated spectral reflectivity curves of the RCE photodiode sample. As desired, a highly reflecting Bragg mirror reflectivity band (1450–1650 nm) and a resonance dip around  $1.55\ \mu\text{m}$  were observed. An excellent agreement between experimental and theoretical results was achieved.

The samples were fabricated by a seven-level microwave-compatible fabrication process in class-100 clean-room environment.<sup>15</sup> The resulting RCE  $p-i-n$  photodiodes had breakdown voltages around 15 V and turn-on voltages around 1 V. Small area devices exhibited a few tens of nA dark current at 1 V reverse bias voltage. Spectral photoresponse of the fabricated devices was measured in the 1500–1600 nm range using a tunable laser source. Figure 2(a) shows the spectral quantum efficiency measurement of an 80- $\mu\text{m}$ -diam RCE photodiode as a function of applied reverse bias voltage. The resonant peak was measured to be around 1548 nm. The peak efficiency increased with reverse bias, mainly due to the enhanced depletion of the active LT-GaAs layer. To compare the efficiency performance of RCE structure with the single-pass structure, single-pass devices were also measured. Figure 2(b) shows the measured and simulated spectral quantum efficiency curves of RCE and single-pass detector samples. The measurements were taken under 3 V reverse bias. The use of resonant cavity has increased the quantum efficiency by a factor of 4.9. The measured enhancement factor was even higher under zero bias

reaching a maximum of 7.5, which was close to the theoretically calculated value of 8.3.

Despite the close agreement between the measured and calculated enhancement factors, there is a huge discrepancy between the experimental and simulated quantum efficiency values. The measured efficiency values were more than two orders of magnitude smaller than the theoretical ones. This result can be attributed to the ultrashort carrier lifetime in the active LT-GaAs layer. With a typical carrier lifetime of  $\sim 150$  fs,<sup>19</sup> only the carriers which are generated very close to the

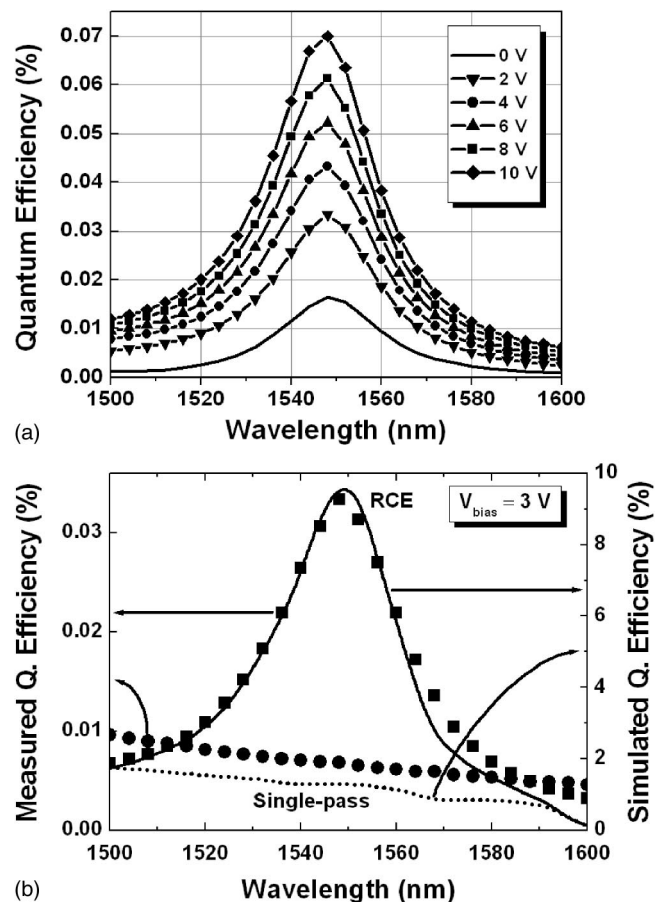


FIG. 2. (a) Measured spectral quantum efficiency of the RCE  $p-i-n$  photodiode as a function of applied reverse bias voltage. (b) Measured (scatters) and simulated (solid and dotted lines) quantum efficiency curves for RCE and single-pass detector samples.

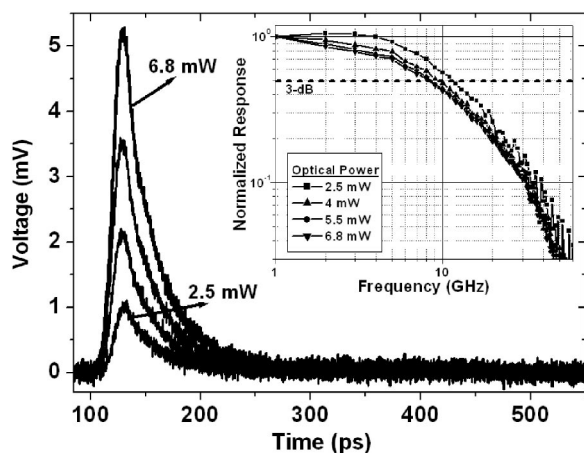


FIG. 3. Temporal pulse responses of a  $7 \times 7 \mu\text{m}^2$  RCE  $p-i-n$  photodiode under different illumination levels at  $1.55 \mu\text{m}$ . Inset shows the calculated FFT curves of the temporal data.

edges of LT-GaAs region can survive the recombination/trapping sites and reach the  $p^+$  or  $n^+$  contact region. We have calculated that only  $\sim 0.45\%$  of all photogenerated carriers contribute to the photocurrent. This collection factor is close to the experimental value of  $\sim 0.35\%$  (Fig. 2). The vast majority of the photogenerated carriers within the LT-GaAs layer cannot reach the contact layers and therefore do not contribute to the photocurrent which results in poor efficiency performance. To increase the carrier collection with longer carrier lifetime, LT-GaAs growth could be done at higher temperatures.<sup>6</sup> However, this results in lower absorption coefficient at the wavelength of interest. This trade-off between carrier lifetime and absorption coefficient limits the long-wavelength efficiency performance of LT-GaAs detector.

High-speed measurements were implemented by utilizing a picosecond fiber laser operating at  $1550 \text{ nm}$ . The  $1 \text{ ps}$  full width-at-half-maximum (FWHM) optical pulses were coupled to the active area of  $p-i-n$  photodiodes by means of a fiber probe. The resulting pulse responses were observed on a  $50 \text{ GHz}$  sampling scope. Faster pulses were measured with smaller devices due to the decreased capacitance and  $RC$  time constant. The pulse response of the detectors was observed to be bias dependent. The pulse amplitude increased with reverse bias due to the enhanced device responsivity. Similarly, as the devices were illuminated at higher optical power levels, stronger pulses were measured. Figure 3 shows the optical power dependence of the temporal high-speed response of a  $7 \times 7 \mu\text{m}^2$  RCE photodiode under zero bias. As the optical power was changed from  $2.5$  to  $6.8 \text{ mW}$ , the rise time increased from  $12$  to  $16 \text{ ps}$ . While the fall time did not change significantly ( $\sim 80 \text{ ps}$ ), larger pulse widths were measured for higher optical power levels. A minimum FWHM of  $30 \text{ ps}$  was measured at  $2.5 \text{ mW}$  illumination. The inset figure shows the corresponding fast Fourier transform (FFT) curves. As the temporal measurements indicated, an inverse proportionality between bandwidth and optical

power was observed. We attribute this behavior to the space-charge screening effect which becomes dominant under high optical illumination conditions.<sup>20</sup> When compared with the theoretically expected transit time or  $RC$  limited response, we postulate that the longer decay times measured are due to slow trap emptying process observed in LT-GaAs.<sup>21</sup> A maximum  $3 \text{ dB}$  bandwidth of  $11.2 \text{ GHz}$  was obtained under  $2.5 \text{ mW}$  illumination. For optical power levels of  $4$ ,  $5.5$ , and  $6.8 \text{ mW}$ ,  $3 \text{ dB}$  bandwidths of  $9.4$ ,  $8.5$ , and  $8.3 \text{ GHz}$  were determined, respectively.

In summary, we have demonstrated  $1.55 \mu\text{m}$  high-speed operation of GaAs-based  $p-i-n$  photodiodes using LT-GaAs absorption layer and RCE detector structure. The device efficiency was enhanced by a factor of  $7.5$  at the resonance wavelength of  $1548 \text{ nm}$ . Temporal high-speed measurements at  $1.55 \mu\text{m}$  resulted in fast pulse responses. Under low-level optical illumination,  $30 \text{ ps}$  pulsewidth and a corresponding  $3 \text{ dB}$  bandwidth of  $11.2 \text{ GHz}$  was achieved.

This work was supported by NATO Grant No. Sfp971970, Turkish Department of Defense Grant No. KOBRA-001, Thales JP8.04, CAM 07N/0059/2002 and "NANOSELF" TIC2002-04096-C03-03. E.O. acknowledges partial support received from Turkish Academy of Sciences.

- <sup>1</sup>J. E. Bowers and Y. G. Wey, in *Handbook of Optics*, edited by M. Bass (McGraw-Hill, New York, 1995), Chap. 17.
- <sup>2</sup>K. Kato, *IEEE Trans. Microwave Theory Tech.* **47**, 1265 (1998).
- <sup>3</sup>I. Kimukin, N. Biyikli, B. Butun, O. Aytur, M. S. Unlu, and E. Ozbay, *IEEE Photonics Technol. Lett.* **14**, 366 (2002).
- <sup>4</sup>A. Srinivasan, K. Sadra, J. C. Campbell, and B. G. Streetman, *J. Electron. Mater.* **22**, 1457 (1993).
- <sup>5</sup>A. C. Warren, J. H. Burroughes, J. M. Woodall, D. T. McInturf, R. T. Hodgson, and M. R. Melloch, *IEEE Electron Device Lett.* **12**, 597 (1991).
- <sup>6</sup>S. Gupta, J. F. Whitaker, and G. A. Mourou, *IEEE J. Quantum Electron.* **28**, 2464 (1992).
- <sup>7</sup>J. F. Whitaker, *Mater. Sci. Eng., B* **22**, 61 (1993).
- <sup>8</sup>P. Grenier and J. F. Whitaker, *Appl. Phys. Lett.* **70**, 1998 (1997).
- <sup>9</sup>Y.-C. Chiu, S. Z. Zhang, S. B. Fleischer, J. E. Bowers, and U. K. Mishra, *Electron. Lett.* **34**, 1253 (1998).
- <sup>10</sup>J.-W. Shi, Y.-H. Chen, K.-G. Gan, Y.-C. Chiu, C.-K. Sun, and J. E. Bowers, *IEEE Photonics Technol. Lett.* **14**, 363 (2002).
- <sup>11</sup>H. S. Loka, S. D. Benjamin, and P. W. E. Smith, *Opt. Commun.* **155**, 206 (1998).
- <sup>12</sup>H. Erlig, S. Wang, T. Azfar, A. Udupa, H. R. Fetterman, and D. C. Streit, *Electron. Lett.* **35**, 173 (1999).
- <sup>13</sup>M. S. Unlu and S. Strite, *J. Appl. Phys.* **78**, 607 (1995).
- <sup>14</sup>M. S. Unlu, M. Gokkavas, B. M. Onat, E. Ata, E. Ozbay, R. P. Mirin, K. J. Knopp, K. A. Bertness, and D. H. Christensen, *Appl. Phys. Lett.* **72**, 2727 (1998).
- <sup>15</sup>E. Ozbay, I. Kimukin, N. Biyikli, O. Aytur, M. Gokkavas, G. Ulu, M. S. Unlu, R. P. Mirin, K. A. Bertness, and D. H. Christensen, *Appl. Phys. Lett.* **74**, 1072 (1999).
- <sup>16</sup>N. Biyikli, I. Kimukin, O. Aytur, M. Gokkavas, M. S. Unlu, and E. Ozbay, *IEEE Photonics Technol. Lett.* **13**, 705 (2001).
- <sup>17</sup>C. Lennox, H. Nie, P. Yuan, G. Kinsey, A. L. Holmes, B. G. Streetman, and J. C. Campbell, *IEEE Photonics Technol. Lett.* **11**, 1162 (1999).
- <sup>18</sup>I. Kimukin, N. Biyikli, B. Butun, O. Aytur, M. S. Unlu, and E. Ozbay, *IEEE Photonics Technol. Lett.* **14**, 366 (2002).
- <sup>19</sup>G. L. Witt, *Mater. Sci. Eng., B* **22**, 9 (1993).
- <sup>20</sup>K.-G. Gan, J.-W. Shi, Y.-H. Chen, C.-K. Sun, Y.-C. Chiu, and J. E. Bowers, *Appl. Phys. Lett.* **80**, 4054 (2002).
- <sup>21</sup>H. S. Loka, S. D. Benjamin, and P. W. E. Smith, *IEEE J. Quantum Electron.* **34**, 1426 (1998).